Dynamic strain aging and the role of the Cottrell atmosphere

I. H. Katzarov*
IMSET, Bulgarian Academy of Sciences, 67 Shipchenski prohod Str., Sofia 1574, Bulgaria
and Department of Physics, King's College London, Strand, London WC2R 2LS, United Kingdom

L. B. Drenchev
IMSET, Bulgarian Academy of Sciences, 67 Shipchenski prohod Str., Sofia 1574, Bulgaria

D. L. Pashov
Department of Physics, King's College London, Strand, London WC2R 2LS, United Kingdom

T. N. A. T. Zarrouk and O. Al-lahham
Department of Physics, King's College London, Strand, London WC2R 2LS, United Kingdom

A. T. Paxton
Department of Materials, Imperial College London, South Kensington Campus, London SW7 2AZ, United Kingdom.

(Received 2 February 2022; revised 27 April 2022; accepted 9 June 2022; published 24 June 2022)

We have developed an atomistic kinetic Monte Carlo (kMC) model describing carbon diffusion, trapping and detrapping in the stress field generated by a 1/2[111] screw dislocation in bcc iron. By performing long time scale carbon diffusion simulations we study the formation of carbon Cottrell atmospheres around screw dislocations at different temperatures and background carbon concentrations. The kMC simulations allow us to predict the rate of formation and strength of carbon atmospheres which control the dislocation's behavior resulting in dynamic strain aging in steel. From the kMC simulations of carbon diffusivity in a block of iron crystal containing a screw dislocation we extract the effective diffusion constants. Our results show that except at low carbon concentrations the diffusivity resulting from carbon transport inside the dislocation core dominates the effective diffusivity, which indicates that pipe diffusion in a screw dislocation is likely. The kMC approach, which explicitly accounts for the behavior of individual carbon atoms, offers an atomistic view of the carbon drag mechanism by which mobile dislocations can collect and transport carbon within their cores. We simulate the carbon drag mechanism at different temperatures, background carbon concentrations, and dislocation velocities and estimate the maximal dislocation velocity at which the atmosphere of carbon atoms can follow a moving screw dislocation.

DOI: 10.1103/PhysRevMaterials.6.063603

I. INTRODUCTION

Steel plasticity is strongly influenced by interactions between solute atoms, such as carbon, and dislocations [1]. An almost unique feature of the plasticity of steel is the role of the Cottrell atmosphere, which results from the trapping of carbon atoms by dislocations. The atmosphere is known to pin dislocations and render them less mobile than otherwise. At any level of carbon concentration above a few parts per million and at any normal dislocation density and ambient temperature it is expected that all dislocations will have trapped carbon atoms. As a result a larger shear stress is required to initiate flow and as the stress is increased three things may happen. The dislocation may break away from its atmosphere; it may drag its atmosphere with it; or new dislocation sources may be activated. Many well known phenomena observed in steel are associated with this: yield drop, serrated yield, stretcher strains and strain aging, for example. It has been suggested that the to and fro motion of dislocations under fatigue loading is responsible for the transport of carbon atoms and the dissolution of carbides leading to microstructural degradation [2]. The atmosphere is indeed the underlying atomistic mechanism behind steel hardening observed during strain aging experiments [3–5].

The hardening of a material that is aged for a certain period of time after undergoing plastic deformation is commonly termed static strain aging. In contrast to static strain aging, which takes place during the specimen rest time, another strain aging phenomenon, called dynamic strain aging occurs during the plastic deformation of a specimen. It is associated with the diffusion of impurities to a mobile dislocation temporarily arrested at obstacles. Dynamic strain aging is responsible for "blue brittleness" in plain carbon steel. The dynamic interaction between mobile dislocations and solute carbon atoms in bcc iron results in dynamic

*ivaylo.katsarov@kcl.ac.uk

strain aging effects in the temperature range of 100°C−300°C [6].

Studying strain aging is a very challenging problem, both theoretically and experimentally, because it spans multiple spatial and temporal scales. One of the purposes of the present theoretical work is to predict the conditions of stress, temperature, and carbon concentration at which a transition may occur between carbon drag and breakaway. We are motivated by recent measurements by Caillard [6] in binary iron–carbon alloys with carbon concentrations of 1, 15, and 50 atomic parts per million (appm). Caillard found three regimes of behavior: (*i*) the expected Peierls mechanism of kink pair formation and migration at low temperature; (*ii*) avalanches of curved dislocations at intermediate temperature corresponding to the observed jerky flow—this giving way at higher temperature to serrated flow—both characterized by periods of quiescence punctuated by avalanches of dislocation glide; (*iii*) above about 200°C a new mechanism was discovered, namely viscous glide accomplished by a Peierls mechanism but with an activation energy almost twice that of the room temperature viscous flow. Caillard also ascertained that dynamical strain aging is caused by the trapping of carbon by straight screw, not edge segments of dislocations in contradiction of the standard explanation in terms of Cottrell atmospheres. For this reason we focus on the long straight screw dislocation in the present work.

Although the underlying atomistic mechanism of strain aging is well established (carbon and other impurities migrate and pin dislocations), many aspects of this important phenomenon remain poorly understood. Recent three-dimensional atom probe techniques permitted the visualization of impurities distributed around dislocations [7–9], providing experimental evidence of Cottrell atmospheres. However, these techniques provide only a static picture of the atmosphere. The impurity diffusion to dislocations and the subsequent Cottrell atmosphere formation remains a challenge for these techniques.

Despite the limitations inherent to mesoscopic approaches applied to an atomistic problem some models, based on classical elasticity theory, were proposed and explained many aspects of strain aging [10–12]. An atomistic view of impurity diffusion near and to dislocations leading to the Cottrell atmosphere formation can be achieved by simulations, where atomistic details are explicitly taken into account [13,14]. Most of exisiting work employs static calculations of carbon-dislocation binding energies to model the equilibrium Cottrell atmosphere around dislocation as a function of the carbon content [4,14–16]. The formation of the Cottrell atmosphere and dislocation unpinning from the resulting carbon cloud, have been simulated with methods that fully take into account the behavior of individual atoms (for example, molecular dynamics, which is the standard method for computer simulations at the atomic scale) [17–19]. However, diffusion in the solid, which is a thermally activated phenomenon, proceeds slowly compared to the typical time scale that can be achieved by molecular dynamics. One of the most promising alternatives is the kinetic Monte Carlo method (kMC). With kMC, computer simulations can even achieve the experimental time scale, while describing accurately the diffusion processes. In Ref. [20] carbon diffusion near the core of an edge and a screw 1/2[111] dislocation in bcc iron was investigated by means of an atomistic kinetic Monte Carlo model (akMC). Molecular statics simulations with an embedded atom method (EAM) potential [21] have been carried out in order to obtain atomic configurations and the activation energies required for carbon hops in the neighborhood of the line defect. The kinetics given by the akMC simulations is a competition between two absorbing barriers—the core region ($R < 4b \approx 1$ nm, b is the Burgers vector) and the outer boundary ($R > 6$ nm) of the simulation box. In the first case, a carbon atom is considered trapped by the dislocation; in the other case, the carbon trajectory simply is not followed anymore. The result of simulated simple random walks permits study of the carbon diffusion near the core of a dislocation but cannot describe the behavior of carbon atoms inside the core and escape from the core region. Simulation of diffusion in the core region of dislocations, where carbon atoms have a different migration energy profile, is necessary for studying dislocation-driven transfer of carbon atoms. It has been suggested [22–24] that diffusion in the core region is higher than diffusivity in the bulk and that dislocations act as accelerated paths (pipes) for carbon diffusion. Another scenario for dislocation-driven transport of carbon atoms is based on the assumption that a mobile dislocation can collect carbon atoms and drag them [2,5]. Recent measurements by Caillard [6] indicate that at intermediate temperatures carbon atoms in bcc iron become sufficiently mobile to move to the nearest dislocations and pin them. This results in the dynamic strain aging effect characterized by a low ductility and high strain hardening. The effect of carbon-dislocation interactions in this temperature domain is characterized by jerky and serrated flow [6]. A dislocation drag mechanism takes place if the diffusion of carbon atoms and the motion of dislocations occur with rates in the same order of magnitude. At high temperatures carbon atoms in bcc iron become mobile enough to follow gliding dislocations. The yield stress and strain hardening decrease with increasing temperature and the ductility increases. The effect of carbon in the high temperature domain is characterized by a low mobility of screw dislocations controlled by a high-temperature Peierls mechanism [6]. The transitions between these domains vary as a function of dislocation velocity, but so far a quantitative analysis has been lacking. To study drag of carbon atoms by dislocations requires simulation techniques that capture carbon diffusion events, trapping and escape from the core and the motion of dislocations simultaneously. The carbon drag mechanism has been previously studied using molecular dynamics simulations [18]. Since the molecular dynamics technique is not capable of simulating the time scales for realistic strain rates, a discrete diffusion method is used in Ref. [25] to overcome the limitations of molecular dynamics simulations. This approach determines the time dependence of the carbon occupation of trap sites by knowing the rates of all escape and trapping jumps calculated by harmonic transition-state-theory but cannot describe the behavior of individual carbon atoms.

In this work we develop an atomistic kinetic Monte Carlo model describing carbon diffusion in the nonhomogeneous stress field created by a 1/2[111] screw dislocation in bcc iron, where the behavior of individual atoms is explicitly taken into account. This kMC model allows us to study both the

diffusing carbon residing in the dislocation core and carbon atoms which move through the interstitial sites in dislocation surroundings. The on-lattice kMC model employs information gathered from molecular statics simulations carried out in order to determine the activation energies required for carbon hops in the neighborhood of the line defect [25]. We employ the present kMC model to simulate carbon diffusion, trapping and detrapping in the stress field generated by a screw dislocation in bcc iron leading to the formation of Cottrell atmosphere. The kMC approach, which explicitly accounts for the behavior of individual carbon atoms, offers an atomistic view of carbon drag mechanism by which mobile dislocations can collect and transport carbon within their cores. We study the carbon drag mechanism at different temperatures, background carbon concentrations, and dislocation velocities.

The structure of the paper is as follows. Section II gives details of the kinetic Monte Carlo model describing carbon diffusion in the surroundings of a 1/2[111] screw dislocation in bcc Fe. Section III is our results and discussion section: In Sec. III A we perform long time scale simulations of carbon diffusion, trapping, and detrapping in the stress field generated by a screw dislocation leading to formation of Cottrell atmosphere. In Sec. III B, we determine the rate of formation and strength of carbon atmospheres which control dislocation behavior resulting in dynamic strain aging in Fe due to various concentrations of carbon solute atoms. Section III C presents our results of the simulated evolution of carbon clouds dragged by a mobile screw dislocation. We conclude in Sec. IV.

II. METHODOLOGY OF MODELING

The kinetic Monte Carlo method exploits the fact that the long-time dynamics of an atomic system typically consists of diffusive jumps from one state to another, separated by an energy barrier, with long periods when particles vibrate in the potential wells of the metastable sites. Molecular dynamics calculations follow the trajectory through every vibrational period while kMC treats directly only the state-to-state transitions. The result is that kMC can reach vastly longer time scales. Even though only one or a few atoms escape over an energy barrier in these cases, kMC does not simply move atoms to new states, the entire system has been taken to a new state. The time step Δt in the kMC model is the time that the system resides in the current state before the next transition. Δt_i depends on the total transition rate $R(i)$ from state i,

$$R(i) = \sum_j J(i, j), \tag{1}$$

where $J(i, j)$ is the transition rate from state i to state j and the sum is over all states accessible by transitions from state i. The system's residence time Δt_i in state i is a random variable selected from the exponential distribution

$$f(\Delta t_i) = R(i) \exp(-R(i)\Delta t_i). \tag{2}$$

Since the total transition rate varies significantly with variations of the dislocation stress field, temperature, and carbon concentration, the difference between the time steps at different states can differ by several orders of magnitude. The kMC methods use information on the energetic barriers to atomic hopping that are completely specified by the matrix of transition rates $J(i, j)$ expressed by the transition-state theory. The following form of transition-rate matrix element provides a physically consistent description of the thermally activated jumps between the metastable states:

$$J(i, j) = \nu \exp\left(-\frac{\Delta E_{ij}}{k_B T}\right), \tag{3}$$

where $\nu = 1.2 \times 10^{13}$ s^{-1} is the attempt frequency for carbon migration [25] and ΔE_{ij} is the energy barrier between the current metastable state i through the saddle point to the adjacent state j. According to harmonic transition state theory [26], the energy barrier for the transition $i \rightarrow j$ is given by the following simple equation:

$$\Delta E_{ij} = E_{sp} - E_i, \tag{4}$$

where E_{sp} is the total energy of the system at the saddle point (i.e., the transition state) and E_i is the total energy of the system at the state i. The kMC method has also the advantage of being computationally less expensive because the interatomic interactions are not computed directly from the electronic structure on the fly as the simulation proceeds. Instead, kMC uses precomputed transition rates along the minimum energy paths (MEPs) between the metastable sites, allowing in this way employment of more precise electronic structure methods for computation of the energy of the physical system and derivation of the transition rates. In the present study we use carbon migration energy barriers in the vicinity of a 1/2[111] screw dislocation in bcc iron calculated in Ref. [25]. The energetic profile of a carbon atom around a screw dislocation was determined by employing the EAM potential [21] and the nudged elastic band (NEB) technique [27]. The NEB method allows determination of the MEP of a carbon atom jumping from one binding site in the vicinity of the dislocation to another one in the neighborhood of the original site. The binding sites of carbon, and their strengths, were determined by tight-binding calculations of carbon-screw dislocation interactions, where the core configuration was constrained to that of an easy core. These were performed using the Fe-C model of Paxton and Elsässer [28]. These calculations followed a method similar to that of Itakura *et al.* [29], by first relaxing a 522 Fe atom dislocated cell, of $1\mathbf{b} = \sqrt{3/2}a_{\rm bcc}$ depth, in a cluster configuration, where atoms within a radius of $R_1 = 6\sqrt{2}a_{\rm bcc}$, were able to relax fully and atoms between R_1 and $R_2 = 7\sqrt{2}a_{\rm bcc}$ were fixed to their positions resulting from the anisotropic elasticity displacements of the central screw dislocation. From the resultant cell, a smaller circular region of 174 atoms, centered on the relaxed screw dislocation, was extracted, and duplicated to reach a depth of $3\mathbf{b}$. In the middle layer of this cell, carbon atoms were placed in 10 octahedral sites surrounding the dislocation core. So that the screw core could not reconfigure, as has been seen in density functional theory (DFT) results of carbon-screw dislocation binding [30], the the three atoms in the top and bottom layers, were fixed in the $z = \langle 111 \rangle$ direction. A charge tolerance of 1×10^{-6} was used for self-consistency, with k-point meshes of $1 \times 1 \times 24$ and $1 \times 1 \times 12$ for the $1\mathbf{b}$ and $3\mathbf{b}$ depth cells, respectively. Details of the calculation of the migration energy profile of carbon may be found elsewhere [25]. The kMC

model incorporates more than 200 energy barriers between carbon metastable sites in the surroundings of the dislocation center. The calculated energy barriers between the binding sites in the dislocation core (region with radius $R \approx 0.6$ nm in the direct neighborhood of the dislocation center) are significantly modified compared to the perfect lattice. The carbon activation energy barriers in the dislocation core surroundings are regular and close in value to the perfect bcc Fe bulk diffusion barrier of 0.86 eV. Of particular importance are the regions in the core called in Ref. [25] the "high-mobility zone", where the carbon diffusion barriers between neighboring binding sites drop to 0.2 eV which is significantly lower than the carbon diffusion barrier in the perfect bcc lattice. These low energy barriers indicate that carbon atoms can be extremely mobile in the core region, which is expected to have implications on pipe diffusion and carbon drag mechanisms. DFT calculations of the carbon-screw dislocation interaction energy at different separation distance between carbon atoms along the dislocation line show a strong repulsion between carbon atoms, which is mostly limited to the first neighbors (carbon-carbon separation of $1b$) [30]. Considering only a first nearest-neighbor interaction between carbon atoms along the dislocation line, the binding energy per carbon atom at site i (calculated by DFT) can be expressed as

$$E(1b)_i = E_i + E_{\mathrm{CC}} + \Delta E_{\mathrm{eh}}, \tag{5}$$

where E_i is the binding energy of an isolated carbon atom, $\Delta E_{\mathrm{eh}} = 0.04$ eV is the energy cost to transform a segment of length $1b$ from easy to hard core and $E_{\mathrm{CC}} = 0.21$ eV is the C–C first-neighbor repulsion term [30]. When the first nearest-neighbor of site i along the dislocation line is occupied we introduce a correction to the transition energy barriers from site i, ΔE_{ij}, used by the kMC model, by replacing the binding energy E_i of an isolated carbon atom in Eq. (4) with the binding energy $E(1b)_i$ calculated in Eq. (5).

III. RESULTS AND DISCUSSION

A. Segregation of carbon around static screw dislocations. Comparison to atom probe data

The binding sites of carbon around an easy screw core are shown in Fig. 1. We see that the binding energy is highly dependent on site position. The E1 and E2 sites closest to the core have some of the largest binding energies of ∼0.79 eV, with the second shell of sites from the core center, E3 and E4 decreasing to 0.14 and 0.24 eV, respectively. It increases for the third shell from the core, to 0.79, 0.60, and 0.69 eV for the E5, E6, and E9 sites, respectively. There was no significant change in the site positions of the carbon upon relaxation of the lattice bar that of the E1 site, which moved away from the core, to a site in the center of an adjoining triangle of atoms to the screw core.

The three-dimensional atomic-scale distribution of carbon atoms around dislocations in bcc iron has been achieved by using position-sensitive atom probe microscopy [8]. Experimental samples have been aged for controlled periods, in excess of 24 h, at room temperature to ensure complete carbon segregation. The Cottrell atmosphere in the atom probe data has been visually identified as impurity enriched zones and extends outwards from the dislocation core to a

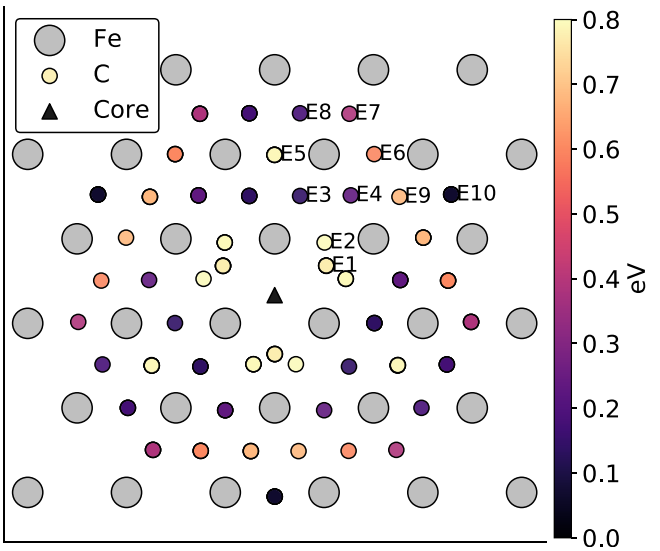

FIG. 1. The binding sites of carbon around an easy $\mathbf{b} = 1/2\langle 111\rangle$ screw core as calculated with tight-binding, where the color denotes the binding energy. The $\langle 111\rangle$ axis goes into the page.

distance of about 7 nm. Wilde *et al.* [8] observed that at background carbon concentration 0.85 at.% about 105 carbon atoms per length of 1 nm of the line defect segregated to form an atmosphere around a dislocation, identified as 1/2[111] screw. The kMC treatment of carbon Cottrell atmosphere formation presented in this work considers a portion of the atmosphere contained inside a fixed volume parallelepipedal region $10 \times 10 \times 10$ nm^3, the rectangular cross section of which (10×10 nm^2) corresponds approximately to the core region of the atom probe experiments. In the present study the parallelepipedal region is in contact with an infinite carbon reservoir, such that no carbon depletion occurs in the matrix due to segregation. The calculations were run for $10^9 - 10^{10}$ kMC steps which is sufficient to represent the steady state. The evolution of the number of carbon atoms segregated to

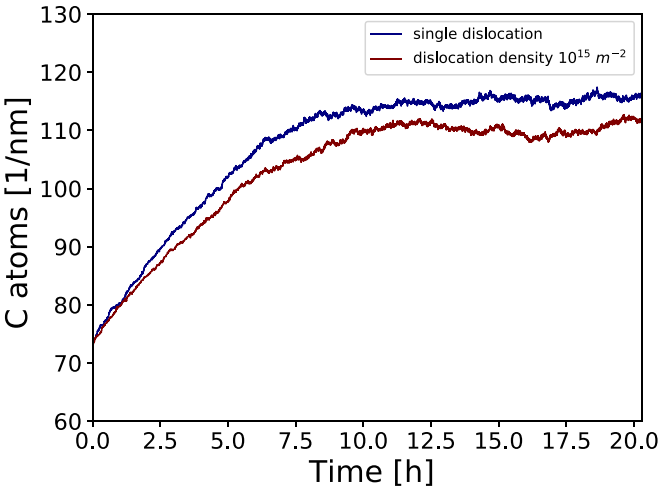

FIG. 2. The evolution of the number of carbon atoms segregated to form an atmosphere around a 1/2[111] screw dislocation at background carbon concentration 0.85 at. %.

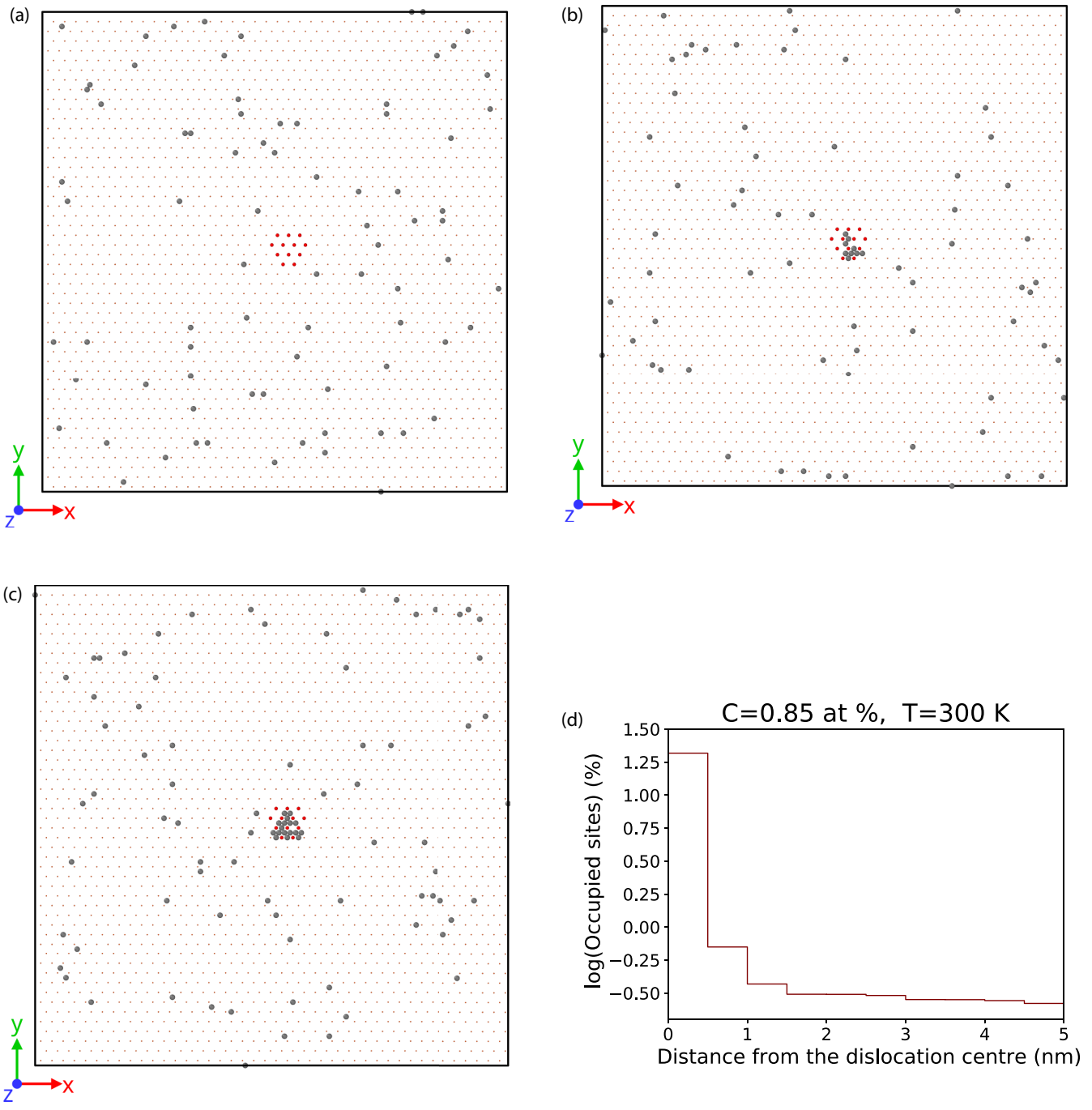

FIG. 3. (a)–(c) The formation of a carbon Cottrell atmosphere illustrated by a series of snapshots. The kMC simulations are carried out at a background carbon concentration of 0.85 at. % and temperature 300 K. The simulation cell is oriented as $X = [11\bar{2}]$, $Y = [1\bar{1}0]$ and $Z = [111]$. The red colored iron atoms designate the core region; (d) the averaged equilibrium carbon concentrations around the screw dislocation.

form an atmosphere around a 1/2[111] screw dislocation at background carbon concentration 0.85 at. % simulated by our kMC model is shown in Fig. 2.

At a temperature of 300 K we find that the carbon atmosphere is formed after aging for a period of about 10 h. After formation of the equilibrium carbon atmosphere the number of carbon atoms varies in the range of 115–118 C/nm. One can see that despite the simplifications of the kMC model the experimental value of 105 C/nm around a screw dislocation is remarkably close to what the present model predicts. Snapshots of the spatial distribution of carbon atoms in $10 \times 10 \times 1$ nm^3 volume during formation of the Cottrell atmosphere around screw dislocation are shown in Figs. 3(a)–3(c). Figure 3(d) shows the ensemble-averaged equilibrium local carbon concentrations around the screw dislocation as a function of the distance from the dislocation center.

Many details of experimental samples are too complex to be taken into account by our kMC model that has to be kept as simple as possible to be applicable. For instance, a realistic

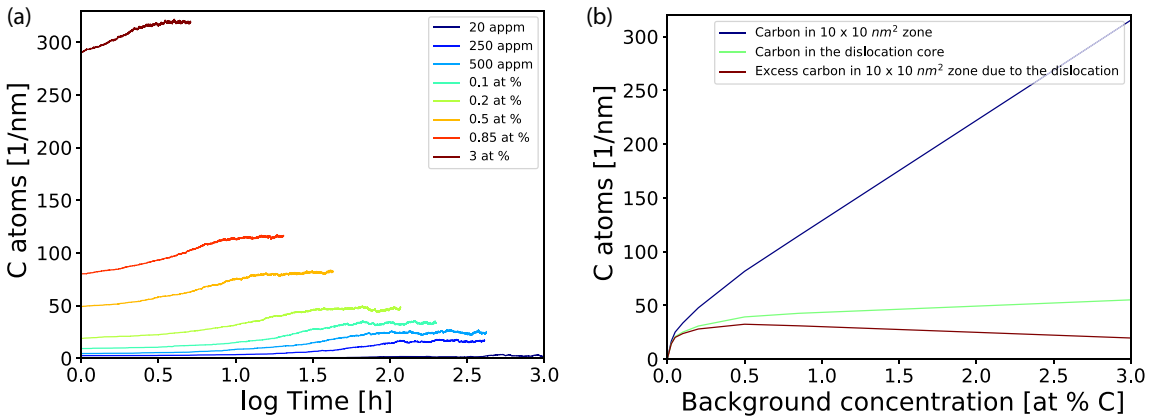

FIG. 4. (a) The evolution of the number of carbon atoms segregated to form an atmosphere around a 1/2[111] screw dislocation at background carbon concentrations in the 20 appm–3 at. % range and temperature 300 K; (b) The number of carbon atoms per 1 nm segregated at steady-state conditions in the 10×10 nm^2 cell, in the core regions and the excess of carbon in the cell as functions of the background carbon concentration.

sample may contain a high density of different kinds and orientations of dislocations and other defects that can act as traps for carbon. The number of carbon atoms inside a fixed volume V far away from a dislocation N_{bulk} is linked to the nominal number of carbon atoms in the same volume of the matrix N_{nom} by matter conservation equation

$$N_{\text{bulk}} = N_{\text{nom}} - \rho N_d V, \tag{6}$$

where N_d is the number of carbon atoms per unit length trapped in the dislocation cores and ρ is the dislocation density. With the help of this relation, we can simulate, self-consistently, the formation of the carbon atmosphere around screw dislocation as a function of the nominal carbon concentration and dislocation density. Figure 2 shows the evolution of the number of segregated carbon atoms forming an atmosphere around screw dislocation at a nominal carbon concentration of 0.85 at. % and dislocation density $\rho = 10^{15}$ m^{-2}. The present model predicts that the number of carbon atoms in the Cottrell atmosphere varies in the range of 109–111 C/nm, which is even closer to the experimental value. We employ our kMC model to simulate the formation of a carbon atmosphere and to determine the number of carbon atoms per 1 nm length of dislocation corresponding to background carbon concentrations in the 20 appm–3 at. % range. The simulated evolution of the number of carbon atoms in the Cottrell atmosphere (the 10×10 nm^2 region surrounding dislocation center) is presented in Fig. 4(a). The time required for the system to reach a steady-state condition decreases with increase of the background carbon concentration. It varies from 4 h at a concentration of 3 at. % to more than 500 h at 20 appm. The number of carbon atoms per 1 nm segregated at steady-state conditions in the 10×10 nm^2 and in the core (region with radius $R \approx 0.6$ nm in the direct neighborhood of the dislocation center [25]) as functions of the background carbon concentration is shown in Fig. 4(b). With increasing background concentration the number of carbon atoms trapped in the dislocation core converges to the saturation limit and the increase of carbon in the Cottrell atmosphere is due to segregation of carbon atoms in the surroundings of the dislocation core. Figure 4(b) also shows the excess of carbon atoms in the $10 \times 10 \times 1$ nm^3 cell due to the presence of the dislocation, which is the number of C atoms in the cell minus the equilibrium density away from the dislocation times the volume of the cell. The excess of carbon atoms as a function of the background carbon concentration has a maximum at 0.5 at. % C.

Dynamic strain aging in iron due to various concentrations of carbon solute atoms has been studied by *in situ* straining experiments in a transmission electron microscope [6]. At 16 appm carbon and 20°C, screw dislocations have a slow and steady motion controlled by the Peierls mechanism. At 100°C, dislocations start to move in bursts—no dislocation motion is observed upon straining during several minutes, until a source is unlocked and emits many dislocations. At 230 appm background carbon concentration the dislocation motion is already in bursts at $T = 20$°C. The observed dislocation behavior is associated with the diffusion of carbon to a temporarily arrested dislocation and the rate of segregation of carbon atoms in the core region. We employ our kMC model to simulate the Cottrell atmosphere formation around a screw dislocation at different temperatures and background carbon concentrations. The kMC simulations allow us to predict the rate of formation and strength of carbon atmospheres.

According to our simulations at 250 appm background carbon concentration and $T = 300$ K the number of carbon atoms trapped in the dislocation core within a period of 3–15 minutes is in the 0.1–0.3 C/nm range [Fig. 5(a)]. At 20 appm and $T = 300$ K no carbon atoms are trapped in the dislocation core for more than 1 h in the initial period of carbon atmosphere formation, according to the kMC simulations. However, with increasing the temperature to 370 K the carbon atoms become more mobile and an equilibrium carbon Cottrell atmosphere is formed over a period of 3–15 minutes when the background carbon concentration is 20 appm. The number of carbon atoms trapped in the dislocation core is in the 0.3–1.3 C/nm range. The comparison between the results of kMC simulations and experimental observations indicates that dynamic strain aging

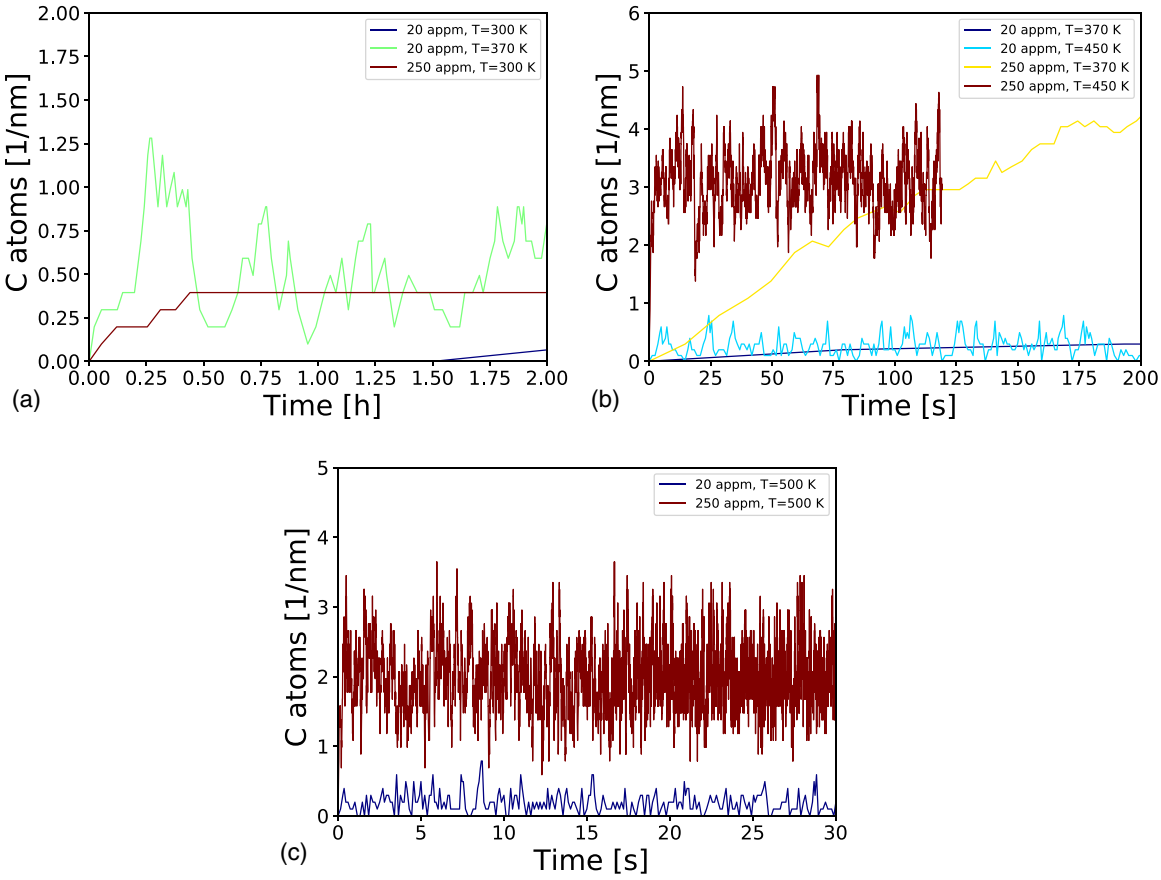

FIG. 5. The number of carbon atoms per 1nm trapped in the dislocation core at different temperatures and background carbon concentrations.

effects start when the background carbon concentration is high enough or carbon atoms become sufficiently mobile to move to the nearest dislocations and form atmospheres of 0.1–0.2 carbon atoms and above per 1 nm while dislocations are temporarily arrested. At $T = 300$ K neither the background concentration of 20 appm nor the mobility of carbon atoms are sufficiently high to form an atmosphere which can pin screw dislocation upon straining during several minutes.

In situ straining experiments [6] reveal that at 16 appm and $T = 200$°C, screw dislocations tend to lock themselves in the pure screw orientation. At 230 appm the straight screw segments are locked, as observed in 16 appm, at $T = 160$°C. The present kMC simulations show that at $T = 450$ K (177°C) and background carbon concentrations of 20 and 250 appm an equilibrium carbon Cottrell atmosphere is formed within a few seconds (5 sec for 20 appm and 1 sec for 250 appm) [Fig. 5(b)]. At equilibrium the average number of carbon atoms trapped in the screw dislocation core is around 0.3 C/nm at 20 appm and 3 C/nm at 250 appm. At 500 K (227°C) the equilibrium carbon Cottrell atmosphere around a screw dislocation is formed even faster—0.4 sec for background carbon concentration of 20 appm and 0.3 sec for 250 appm [Fig. 5(c)]. The kMC calculations indicate that dislocation locking in the pure screw orientation around 160°C at 230 appm and 200°C at 16 appm can be attributed to the strong interaction between carbon atoms and the screw components, resulting from the rapid trapping of carbon atoms in the dislocation core. In this case the diffusion of carbon to a temporarily arrested mobile screw dislocation almost immediately forms a Cottrell cloud which hinders dislocation motion.

B. Diffusivity around screw dislocations; pipe diffusion

One of the proposed mechanisms for carbon redistribution suggests that dislocations located in the ferrite phase and crossing the ferrite-cementite interface act as pipes for carbon diffusion from cementite to the ferrite. As shown in Ref. [25], the diffusion barriers of carbon in the vicinity of a screw dislocation are significantly reduced in the high-mobility zone (region close to the dislocation center). This can be considered as an indication that the diffusion in the core region could be faster than in the bulk region and dislocations can act as accelerated paths for carbon diffusion. In the present study we employ kMC to simulate carbon diffusivity in a block of iron crystal containing a screw dislocation and from the evolution of the simulations we extract an effective diffusivity. The kMC treatment of carbon diffusivity around a screw dislocation considers a portion of the carbon atmosphere contained inside a fixed volume parallelepipedal region $10 \times 10 \times 10$ nm^3. The diffusion coefficient D can be determined from a kMC calculation by employing the Einstein expression

$$D = \lim_{t\to\infty} \frac{1}{6t} \langle [r(t) - r(0)]^2 \rangle, \tag{7}$$

where $\langle [r(t) - r(0)]^2 \rangle$ is the average squared displacement of particles in time t, Ref. [31]. Following Refs. [32,33] we measure the diffusion constant $D_i = \frac{1}{6t_i} \langle [r(t_i) - r(0)]^2 \rangle$ over successive kMC steps of time t_i and average this over the entire simulation. During the simulations, we also followed separately carbon diffusion paths in the dislocation core and in the region beyond the dislocation core (R > 0.6 nm). We employ the Einstein expression to calculate and compare the effective diffusion coefficient D_{eff}, the diffusion constants in the surroundings of the dislocation core D_b and within the dislocation core D_c. D_{eff}, D_c, and D_b for a given temperature and carbon concentration have been obtained from the mean square displacements using Einstein's relation Eq.(7) in one simulation. For determination of D_b and D_c we take into account only the diffusion paths in the lattice and in the core region, respectively. All diffusion paths, including the jumps between the core and the surroundings, contribute to determination of the effective diffusion coefficient D_{eff}. The simulations have been run for $10^8 - 10^9$ KMC steps until diffusion coefficients are no longer changing to within a tolerance, which is typically 0.01% of the diffusion constant magnitude. In order to evaluate pipe diffusion we also study and compare the diffusivity along the [111] direction within the dislocation core and in the bulk region beyond the dislocation core. We calculate diffusion constants $D_{\text{eff}}^{[111]}$, $D_b^{[111]}$, and $D_c^{[111]}$ where the corresponding jump paths in Eq.(7) are replaced by their components projected onto the dislocation line. In the direct neighborhood of the dislocation center EAM calculations [25] predict the existence of potential basins that encompass several binding sites. The barriers between the binding sites in a basin are of the order of 0.2 eV, which is significantly lower than the carbon diffusion barrier in perfect bcc bulk. These low diffusion barriers indicate that carbon atoms can be exceptionally mobile in the basins. Since the binding sites in a basin are close together and the basins are separated from the neighboring binding sites by higher energy barriers, it is more appropriate to regard these basins as single binding sites. Therefore, in our kMC calculations of the diffusion constants we do not account for the vibrations of carbon atoms between the binding sites within the basins.

The calculated diffusion coefficients at different temperatures and background carbon concentrations are shown in Figs. 6. At carbon concentration of 20 appm and at temperatures higher than 400 K the diffusivity in the core is lower than diffusivity in the bulk region surrounding the dislocation core [Fig. 6(a)]. At lower temperatures and carbon concentration of 20 appm the majority of the carbon atoms contained inside the kMC simulation volume are trapped in the dislocation core where jump paths have a lower diffusion barrier and the effective diffusivity is dominated by core diffusion. With increasing temperature the carbon atoms frequently escape from the core region which results in the low barrier paths inside the core having less effect on the diffusivity. In its turn the lower number of carbon atoms trapped in the core reduces blocking of the diffusion paths. The above effects in combination with the corresponding jump rates between the binding sites and carbon-carbon repulsion control C diffusivity in the dislocation core. Our kMC calculations of the diffusion coefficients for background carbon concentration in 250 appm to 3 at. % range show that diffusivity in the core region increases and exceeds diffusivity in the surroundings of the dislocation core [Fig. 6(b)]. Diffusivity in the dislocation core increases with increasing background carbon concentration [Figs. 6(b) and 6(c)]. Increasing carbon concentration increases the probability for occurrence of the repulsive configuration when two carbon atoms are at a distance 1b along the dislocation line. This configuration is less stable which increases the carbon diffusivity because carbon atoms migrate to find more stable interstitial positions in the dislocation core. The same dependences are valid for the [111] components of the diffusion constants [Figs. 6(c) and 6(d)]. Thus, our results indicate that except at very low carbon concentrations the diffusivity resulting from carbon transport inside the dislocation core dominates the effective diffusivity in a block of iron crystal containing a screw dislocation. Although diffusion of the carbon atoms in the core region is predominantly in the plane normal to the dislocation line the resulting diffusivity parallel to the dislocation line exceeds the diffusivity along the [111] direction in the dislocation core surroundings. Based on a qualitative analysis of the energy barriers and diffusion paths of a single carbon atom in the screw dislocation core Nematollahi *et al.* [25] conclude that diffusion along the dislocation axis "seems inefficient." In agreement with Ref. [25] our kMC simulations show that at low carbon concentrations diffusivity in the dislocation core is lower compared to diffusion in the dislocation surroundings. However, our kMC simulations indicate that with increasing background carbon concentration diffusivity in the core exceeds the diffusivity in dislocation surroundings and pipe diffusion becomes likely.

The diffusion coefficients calculated according to Eq. (7) characterizes self-diffusivity which takes place under equilibrium. Chemical diffusion occurs in the presence of a concentration gradient. This diffusion is a nonequilibrium process, increases the system entropy, and brings the system closer to equilibrium. Calculation of chemical diffusion coefficient by considering the concentration dependent activity coefficient of carbon is beyond the scope of the present paper. However, in order to study the carbon diffusivity at nonuniform carbon concentration we have considered a $10 \times 10 \times 10$ nm^3 volume surrounding a screw dislocation. Half of the volume along the dislocation line contains 0.85 at. % carbon concentration which is in equilibrium with the carbon atoms trapped in the dislocation core. The rest of the volume contains pure solvent [Fig. 7(a)]. We then ran kMC simulations of carbon diffusion which brings the system close to equilibrium (Fig. 7). We calculated the carbon fluxes in the dislocation core and in dislocation surroundings across the area dividing high and low concentration zones. The calculated average carbon fluxes in the dislocation core and in dislocation surrounding are correspondingly 6.86×10^{-3} and 5.39×10^{-5} $(C/s.nm^2)$. These kMC simulations of chemical diffusion also indicate that screw dislocations can act as diffusion short circuits because the mobility of atoms along such a defect is higher than in the lattice.

The present kMC model cannot reproduce all details of the reconstruction of the energy landscape arising from the segregation of carbon atoms into the dislocation core and the related transformation from easy-core to hard-core configurations predicted by DFT [30]. A similar kMC model,

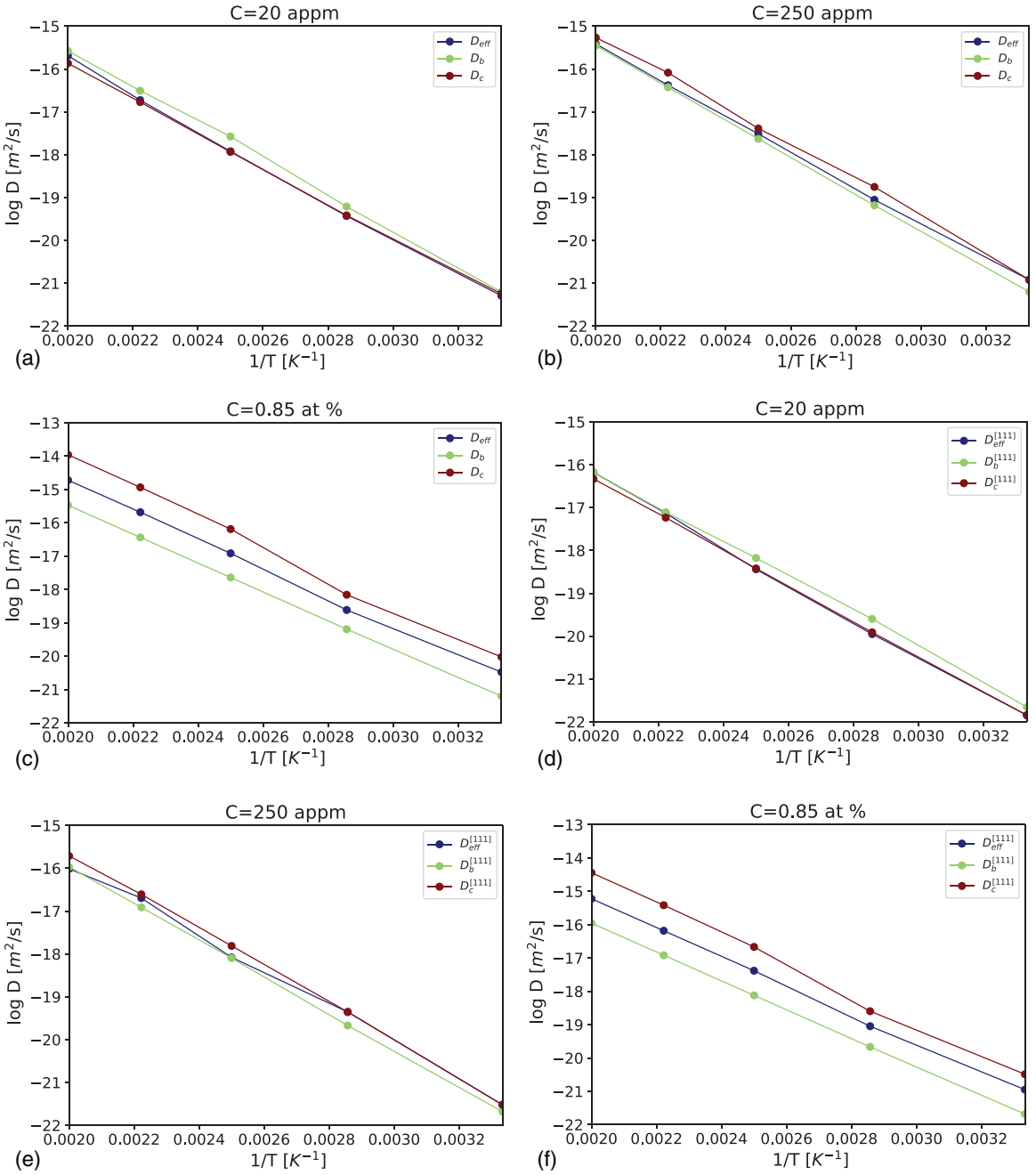

FIG. 6. The calculated diffusion coefficients at different temperatures and background carbon concentrations: (a), (b), and (c) Effective diffusivity and its components in the core and in the surroundings of the core; (d), (e), and (f) [111] components of the diffusion constants

employing migration energy barriers calculated using EAM potential and which does not account for the transformation from easy to hard-core configurations, has been developed to describe hydrogen diffusion and trapping in the stress field generated by the 1/2[111] screw dislocation in bcc iron [33]. The simulated hydrogen diffusion clearly indicates that the diffusivity resulting from hydrogen transport in the core region is several orders of magnitude lower compared to the effective lattice diffusivity and that dislocation lines do not act as fast pathways for hydrogen pipe diffusion [33]. In contrast, the results of our present kMC simulations indicate that the carbon pipe diffusion in screw dislocation is likely. Development of a kMC model accounting for transformations between easy and hard-core configurations resulting from the alteration of carbon occupancy of the binding sites is beyond the scope of the present study.

C. Carbon dragged by a mobile screw dislocation

The carbon drag mechanism suggests that carbon atoms can be transported by mobile dislocations. Due to the strong attractive carbon binding region in the core it is, in principle, possible for screw dislocations to collect carbon atoms and to redistribute them. In order to be able to follow the dislocation, the carbon atoms trapped in the core need to diffuse at least as fast as the dislocation moves. In this section we estimate

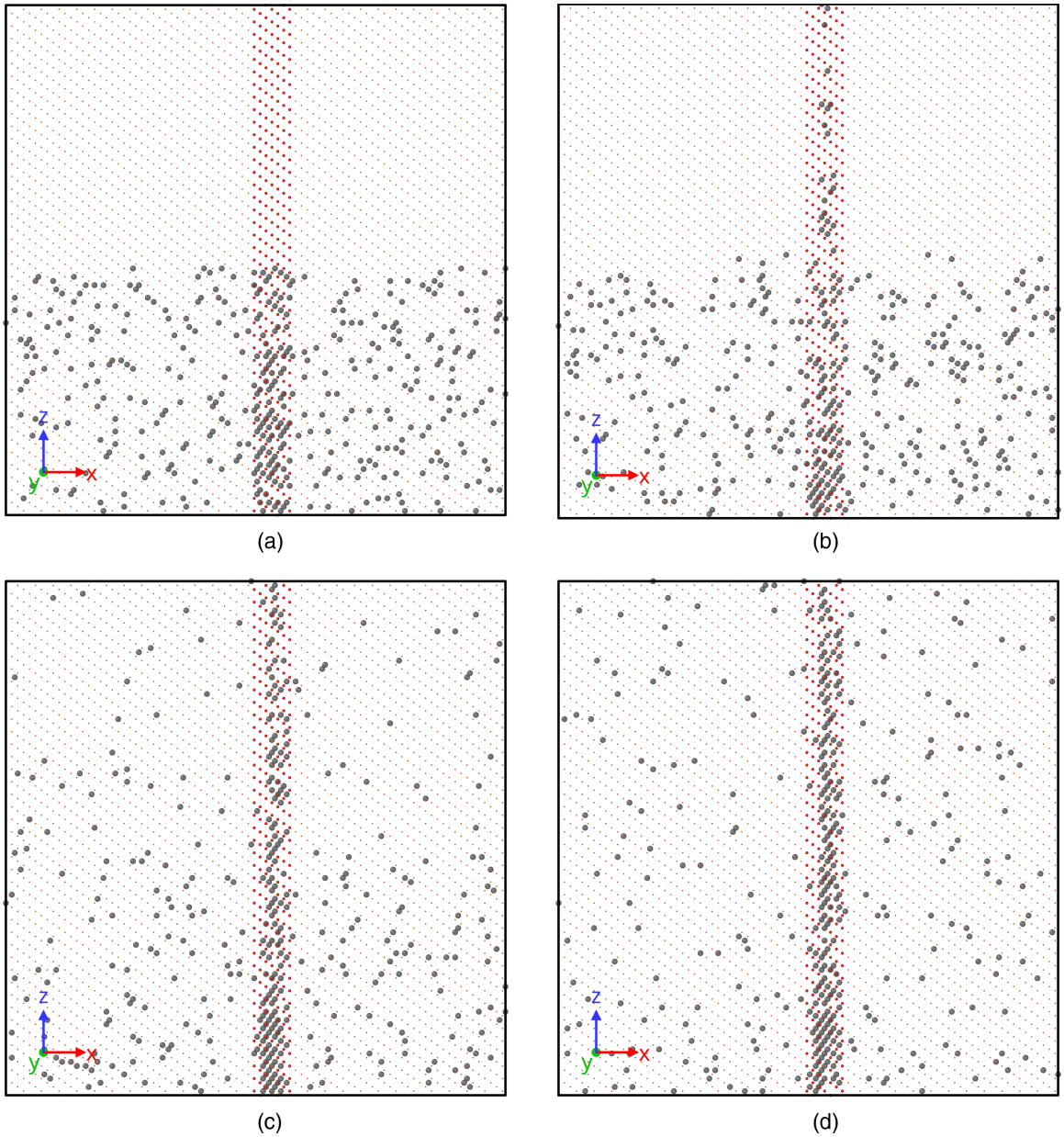

FIG. 7. kMC simulations of the carbon diffusion in a volume with initially nonuniform C concentration illustrated by a series of snapshots. The simulations are carried out at a temperature 300 K.

the velocity with which a carbon atmosphere can follow a moving dislocation. We present our simulation results based on the kMC model allowing us to simulate the migration behavior at experimentally relevant time scales. The kMC treatment of the carbon drag mechanism presented in this section considers the evolution of the carbon cloud dragged by a mobile straight screw dislocation inside a fixed volume parallelepipedal region $60 \times 10 \times 10$ nm^3. At the starting time $t = 0$, the carbon atoms segregated to form an atmosphere around the $1/2[111]$ screw dislocation are at equilibrium with the background carbon concentration. We employ the kMC model to simulate the redistribution of carbon atoms when dislocation migrates in the [110] glide plane with constant velocity v_{dis} (Fig. 8). Carbon atoms trapped in the core can follow the dislocation if it glides slowly and viscously via a Peierls mechanism, namely the process of kink pair creation followed by kink migration. We do not consider kink pair formation and migration explicitly in our simulations. v_{dis} is the velocity of a long straight dislocation moving uniformly between Peierls valleys averaged over the multitude of the kink-pair creation and separation processes.

The resting time between two successive stable kink-pair nucleation steps which move the screw dislocation into an adjacent Peierls valley is much longer than the time required for each of the individual transition steps. Hence, in the present work we assume that carbon transport occurs only in the resting period between the successive jumps. The number of carbon atoms effectively dragged by the dislocation as a function of the dislocation travel distance is shown in Fig. 9 for different dislocation velocities and temperatures. We observe that at background carbon concentrations of 20 and 250 appm more carbon atoms can be transported by the

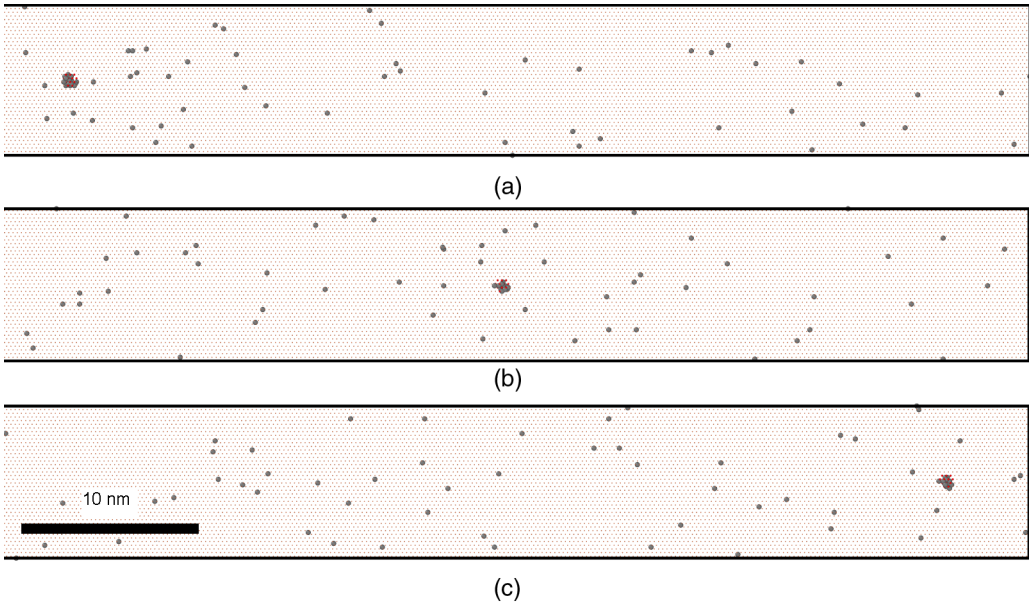

FIG. 8. The motion of a screw dislocation dragging carbon illustrated by a series of snapshots. KMC simulations are carried out at dislocation velocity $v_{dis} = 0.1$ nm/s and temperature 400 K.

dislocation either at lower velocities or at higher temperatures. In particular we estimate the maximal dislocation velocity $v_{\max}$ at which the atmosphere of carbon atoms can follow a moving screw dislocation (Fig. 10). At lower dislocation velocities the carbon atoms have sufficient time to follow the dislocation even at lower temperatures [Figs. 9(a) and 9(b)]. At higher temperatures carbon has a sufficiently high mobility to keep up with faster dislocations [Figs. 9(c) and 9(d). When dislocation velocity is higher than $v_{\max}$ dislocations gradually break away from the carbon clouds. There is a clear dependence of $v_{\max}$ on the background carbon concentration in the 400–450 K temperature range, where $v_{\max}$ at 20 appm is an order of magnitude lower than $v_{\max}$ estimated at 250 appm. At higher background carbon concentration moving dislocations can collect more carbon atoms from the surrounding bulk region. At 500 K our kMC model predicts that $v_{\max}$ has the same magnitude at carbon concentrations of 20 and 250 appm [Figs. 9(e) and 9(f)].

In situ straining experiments [6] reveal that at 16 appm carbon in bcc iron and $T = 250°$C and above the straight screw dislocations start to glide slowly and viscously via a high-temperature Peierls mechanism similar to that observed at 20°C. At carbon concentration of 230 appm and $T = 180°C$ and above the straight screw dislocation motion is controlled by the same high-temperature Peierls mechanism as in 16 appm carbon.

The trapped solute atoms strongly modify the kink pair formation enthalpy E_{kp}, which for a given resolved shear stress is a function of the solute concentration and the rate at which impurities are distributed among trap sites [34]. At lower solute atom mobility the impurities remain behind in binding sites of higher potential energy as a dislocation segment moves between Peierls valleys, leading to a higher Peierls barrier and E_{kp}. The Peierls barrier becomes smaller as the rate at which solute atoms are distributed among trap sites increases [34]. With increasing temperature, the number of solute atoms trapped in the core decreases, which also reduces the Peierls barrier [35]. Hence, as temperature increases E_{kp} decreases as a consequence of the decreasing Peierls barrier.

It could be expected that a screw dislocation can glide via a high-temperature Peierls mechanism if: (a) the kink-pair formation energy barrier, E_{kp}, becomes smaller as the mobility of carbon atoms trapped in dislocation core increases at high temperature; (b) the carbon Cottrell atmosphere can follow the dislocation, that is, a dislocation's average velocity at given carbon concentration and temperature is lower than $v_{\max}$.

At 450 K, the temperature at which dislocations start to glide via a high-temperature Peierls mechanism at carbon concentration of 230 appm, our kMC simulations show that the diffusion coefficient at 250 appm in the dislocation core is $D_c = 5.42 \times 10^{-17}$ m^2/s and $v_{\max} = 1$ nm/s. The experimentally observed average dislocation velocity at 230 appm is 0.04 nm/s at $T = 180°$C and 0.27 nm/s at $T = 200°$C [6]. *In situ* straining experiments reveal that at 16 appm screw dislocations start to glide slowly and viscously at a significantly higher temperature—$T = 250°$C. In accordance with the experimental observations the present kMC simulations at 20 appm and 450 K predict significantly lower core diffusivity and $v_{\max}$ than the same variables calculated at 250 appm—$D_c = 1.69 \times 10^{-17}$ m^2/s and $v_{\max}$=0.1 nm/s. The lower core diffusivity and $v_{\max}$ indicate that the high-temperature Peierls mechanism at 20 appm and 450 K is most probable in a narrower interval of stresses compared to the 250 appm case. The probability of dislocation glide via a high-temperature Peierls mechanism at carbon concentration of 20 appm increases at $T = 500$ K where diffusivity increases to $D_c = 6.66 \times 10^{-22}$ m^2/s and $v_{\max} = 10$ nm/s. The experimentally observed average screw velocity at 16 appm and $T = 250°$C is 7 nm/s [6].

If E_{kp} is small then kink pair formation is easy on all three [110] glide planes, and this leads to increased likelihood of

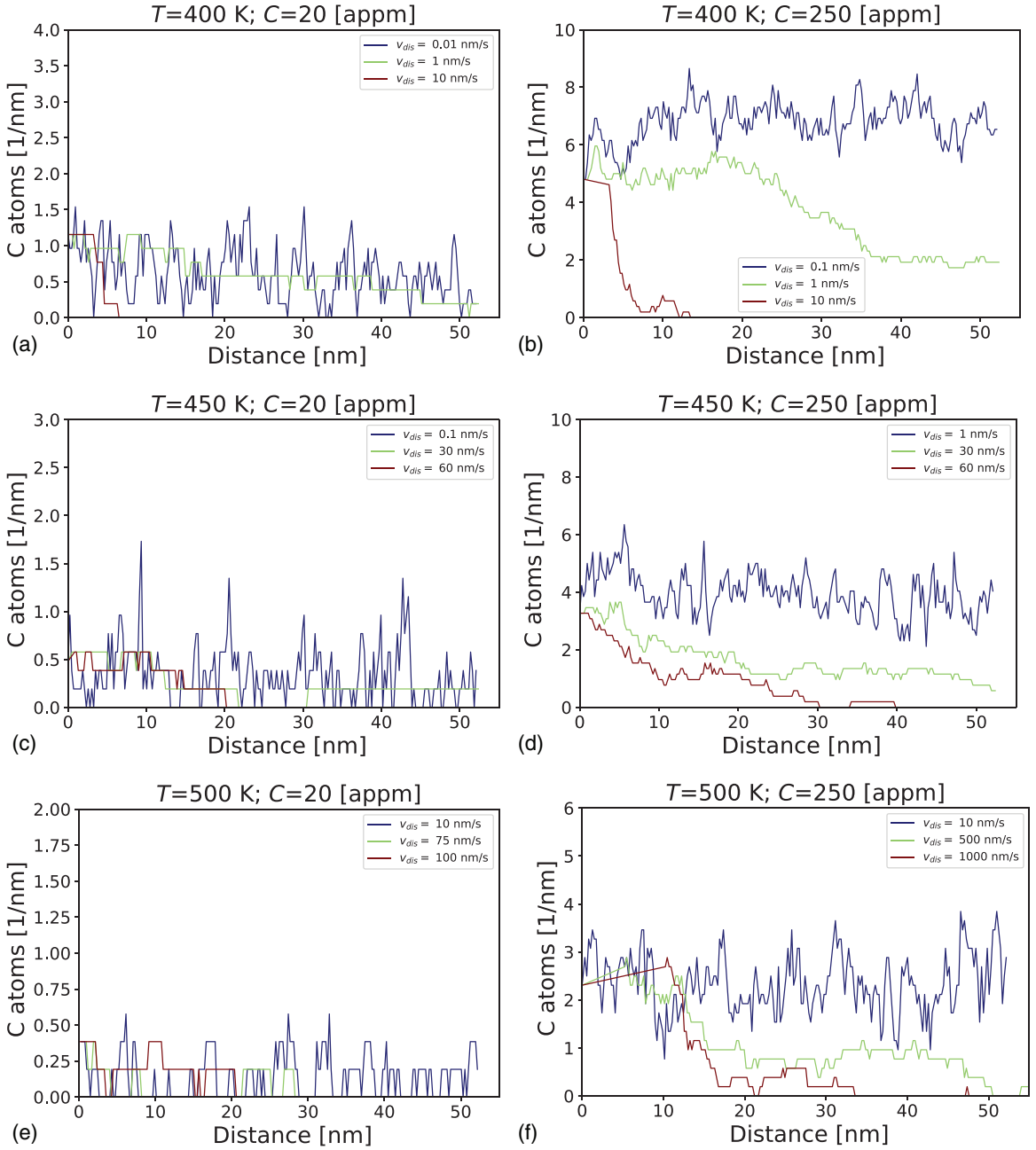

FIG. 9. The evolution of the number of carbon atoms per 1 nm trapped in the core of a moving straight dislocation as a function of the travel distance.

kink pair collisions resulting in the formation of jogs [34,35]. Such jogs amount to self-pinning points which drag out edge dipoles and reduce dislocation mobility. E_{kp} in its turn also depends on the transformations between easy and hard-core configurations resulting from the segregation of carbon atoms into dislocation core. The present kMC model does not take into account the effects of jog formation and self pinning on the dislocation mobility and carbon drag.

IV. CONCLUSIONS

(i) We have developed an atomistic kinetic Monte Carlo model describing carbon diffusion in the nonhomogeneous stress field created by 1/2[111] screw dislocation in bcc iron The kMC model incorporates more than 200 energy barriers between carbon binding sites in the surroundings of the dislocation center determined from molecular statics simulations.

(ii) The number of segregated carbon atoms forming a Cottrell atmosphere around a 1/2[111] screw dislocation, predicted by performing long time kMC simulations, has been validated against the carbon atmosphere visually identified by position-sensitive atom probe microscopy.

(iii) We have simulated the formation of a carbon Cottrell atmosphere around a static screw dislocation and determined the time required for the system to reach a steady-state condition at various background carbon concentrations in the 20 appm–3 at. % range.

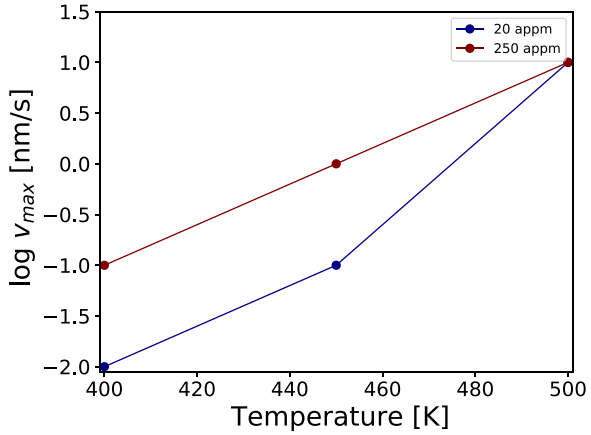

FIG. 10. The maximal dislocation velocity $v_{\max}$ at which the atmosphere of carbon atoms can follow a moving screw dislocation at different temperatures and background carbon concentrations.

(iv) We have also employed our kMC model to simulate the diffusion and segregation of carbon in the core of temporarily arrested screw dislocations at different temperatures and background carbon concentrations. We determine the rate of formation and strength of carbon atmospheres which control dislocation behavior resulting in dynamic strain aging in α iron. Recent experimental studies of DSA in binary iron–carbon alloys indicate that the observed dislocation behavior is associated with the diffusion of carbon to temporarily arrested dislocations, but until now a quantitative analysis has been lacking.

(v) We have applied kMC to simulate carbon diffusivity in a block of iron crystal containing a screw dislocation and determined an effective diffusion coefficient. We also consider separately the carbon diffusion paths in the dislocation core and in the region surrounding the dislocation core. The calculated diffusion coefficients at different temperatures and carbon concentrations in the 20 appm–3 at. % range show that only at low carbon concentration of 20 appm the diffusivity in the core is lower than diffusivity in the bulk region surrounding the dislocation core. Thus, our results show that except at low carbon concentrations the diffusivity resulting from carbon transport inside the dislocation core dominates the effective diffusivity and the probability for occurence of pipe diffusion increases with increasing background carbon concentration

(vi) The kMC approach offers an atomistic view of the carbon drag mechanism by which mobile dislocations can collect and transport carbon within their cores. We have studied the carbon drag mechanism at different temperatures, background carbon concentrations and dislocation velocities. One of the purposes of the kMC simulations is to predict the conditions of temperature T and carbon concentration c_C at which a transition may occur between carbon drag and breakaway. We estimate the maximal dislocation velocity $v_{\max}(T, c_C)$ at which the atmosphere of carbon atoms can follow a moving screw dislocation. We consider $v_{\max}(T, c_C)$ as a limit above which screw dislocations break away from the carbon clouds and cannot glide slowly and viscously. The average velocities of the dislocations gliding via a high-temperature Peierls mechanism, experimentally observed in Ref. [6], are in the range $(0, v_{\max}(T, c_C))$ predicted by our kMC model.

ACKNOWLEDGMENTS

This research was supported in part by the Bulgarian Science Fund under the National Scientific Program "Petar Beron i NIE" (Project UMeLaMP), UKRI Grant No. EP/V001787/1 and by the European Regional Development Fund, within the Operational Programme "Science and Education for Smart Growth 2014–2020" under the Project CoE "National centre of mechatronics and clean technologies" BG05M20P001-1.001-0008-C08. UKRI is aknowledged under the Doctoral Training Partnership for awards to O.A.-l. and T.N.A.T.Z.; and we are grateful to Rolls-Royce plc for a CASE award to T.N.A.T.Z.

[1] D. Caillard, An *in situ* study of hardening and softening of iron by carbon interstitials, Acta Mater. **59**, 4974 (2011).
[2] H. Fu, W. Song, E. I. Galindo-Nava, and P. E. J. Rivera-Díaz-del-Castillo, Strain-induced martensite decay in bearing steels under rolling contact fatigue: Modelling and atomic-scale characterisation, Acta Mater. **139**, 163 (2017).
[3] A. H. Cottrell and B. A. Bilby, Dislocation theory of yielding and strain ageing of iron, Proc. Phys. Soc. A **62**, 49 (1949).
[4] E. Clouet, S. Garruchet, H. Nguyen, M. Perez, and C. S. Becquart, Dislocation interaction with C in α-Fe: A comparison between atomic simulations and elasticity theory, Acta Mater. **56**, 3450 (2008).
[5] Y. Li, P. Choi, C. Borchers, S. Westerkamp, S. Goto, D. Raabe, and R. Kirchheim, Atomic-scale mechanisms of deformation-induced cementite decomposition in pearlite, Acta Mater. **59**, 3965 (2011).
[6] D. Caillard, Dynamic strain ageing in iron alloys: The shielding effect of carbon, Acta Mater. **112**, 273 (2016).
[7] D. Blavette, E. Cadel, A. Fraczkiewicz, and A. Menand, Three-dimensional atomic-scale imaging of impurity segregation to line defects, Science **286**, 2317 (1999).
[8] J. Wilde, A. Cerezo, and G. D. W. Smith, Three-dimensional atomic-scale mapping of a Cottrell atmosphere around a dislocation in iron, Scr. Mater. **43**, 39 (2000).
[9] M. K. Miller, Atom probe tomography characterization of solute segregation to dislocations, Microsc. Res. Tech. **69**, 359 (2006).
[10] N. Louat, The effect of temperature on Cottrell atmospheres, Proc. Phys. Soc. B **69**, 459 (1956).
[11] D. N. Beshers, On the distribution of impurity atoms in the stress field of a dislocation distribution, Acta Metall. **6**, 521 (1958).
[12] A. W. Cochardt, G. Shoek, and H. Wiedersich, Interaction between dislocations and interstitial atoms in body-centered cubic metals, Acta Metall. **3**, 533 (1955).
[13] A. Ramasubramaniam, M. Itakura, M. Ortiz, and E. A. Carter, Effect of atomic scale plasticity on hydrogen diffusion in iron: Quantum mechanically informed and on-the-fly kinetic Monte Carlo simulations, J. Mater. Res. **23**, 2757 (2008).
[14] R. G. A. Veiga, M. Perez, C. S. Becquart, C. Domain, and S. Gar-ruchet, Effect of the stress field of an edge dislocation on carbon diffusion in α-iron: Coupling molecular statics

and atomistic kinetic Monte Carlo, Phys. Rev. B **82**, 054103 (2010).

[15] E. Clouet, Dislocation core field. I. Modeling in anisotropic linear elasticity theory, Phys. Rev. B **84**, 224111 (2011).

[16] R. G. A. Veiga, M. Perez, C. S. Becquart, and C. Domain, Atomistic modeling of carbon Cottrell atmospheres in bcc iron, J. Phys.: Condens. Matter **25**, 025401 (2013).

[17] R. G. A. Veiga, H. Goldenstein, M. Perez, and C. S. Becquart, Monte Carlo and molecular dynamics simulations of screw dislocation locking by Cottrell atmospheres in low carbon Fe–C alloys, Scr. Mater. **108**, 19 (2015).

[18] K. Tapasa, Y. N. Osetsky, and D. J. Bacon, Computer simulation of interaction of an edge dislocation with a carbon interstitial in α-iron and effects on glide, Acta Mater. **55**, 93 (2007).

[19] Y. N. Osetsky and D. J. Bacon, An atomic-level model for studying the dynamics of edge dislocations in metals, Modell. Simul. Mater. Sci. Eng. **11**, 427 (2003).

[20] R. G. A. Veiga, M. Perez, C. S. Becquart, E. Clouet, and C. Domain, Comparison of atomistic and elasticity approaches for carbon diffusion near line defects in α iron, Acta Mater. **59**, 6963 (2011).

[21] C. S. Becquart, J. M. Raulot, G. Bencteux, C. Domain, M. Perez, S. Garruchet, and H. Nguyen, Atomistic modeling of an Fe system with a small concentration of C, Comput. Mater. Sci. **40**, 119 (2007).

[22] M. Legros, G. Dehm, E. Arzt, and T. J. Balk, Observation of giant diffusivity along dislocation cores, Science **319**, 1646 (2008).

[23] E. W. Hart, On the role of dislocations in bulk diffusion, Acta Metall. **5**, 597 (1957).

[24] X. Sauvage and Y. Ivanisenko, The role of carbon segregation on nano- crystallisation of pearlitic steels processed by severe plastic deformation, J. Mater. Sci. **42**, 1615 (2007).

[25] Gh. Ali Nematollahi, B. Grabowski, D. Raabe, and J. Neugebauer, Multiscale description of carbon-supersaturated ferrite in severely drawn pearlitic wires, Acta Mater. **111**, 321 (2016).

[26] G. H. Vineyard, Frequency factors and isotope effects in solid state rate processes, J. Phys. Chem. Solids **3**, 121 (1957).

[27] G. Henkelman and H. Jónsson, Improved tangent estimate in the nudged elastic band method for finding minimum energy paths and saddle points, J. Chem. Phys. **113**, 9978 (2000).

[28] A. T. Paxton and C. Elsässer, Analysis of a carbon dimer bound to a vacancy in iron using density functional theory and a tight binding model, Phys. Rev. B **87**, 224110 (2013).

[29] M. Itakura, H. Kaburaki, M. Yamaguchi, and T. Okita, The effect of hydrogen atoms on the screw dislocation mobility in bcc iron: A first-principles study, Acta Mater. **61**, 6857 (2013).

[30] L. Ventelon, B. Lüthi, E. Clouet, L. Proville, B. Legrand, D. Rodney, and F. Willaime, Dislocation core reconstruction induced by carbon segregation in bcc iron, Phys. Rev. B **91**, 220102(R) (2015).

[31] A. Einstein, On the movement of small particles suspended in a stationary liquid demanded by the molecular-kinetic theory of heat, *Investigations on the Theory of the Brownian Movement* (Dover, New York, 1956).

[32] R. Kirchheim, Hydrogen solubility and diffusivity in defective and amorphous metals, Prog. Mater. Sci. **32**, 261 (1988).

[33] D. Bombac, I. H. Katzarov, D. L. Pashov, and A. T. Paxton, Theoretical evaluation of the role of crystal defects on local equilibrium and effective diffusivity of hydrogen in iron, Mater. Sci. Technol. **33**, 1505 (2017).

[34] P. Gong, I. H. Katzarov, J. Nutter, A. T. Paxton, and W. Mark Rainforth, The influence of hydrogen on plasticity in pure iron—theory and experiment, Sci. Rep. **10**, 10209 (2020).

[35] I. H. Katzarov, D. L. Pashov, and A. T. Paxton, Hydrogen embrittlement I. Analysis of hydrogen-enhanced localized plasticity: Effect of hydrogen on the velocity of screw dislocations in α-Fe, Phys. Rev. Materials **1**, 033602 (2017).